

This item is likely protected under Title 17 of the U.S. Copyright Law. Unless on a Creative Commons license, for uses protected by Copyright Law, contact the copyright holder or the author.

Access to this work was provided by the University of Maryland, Baltimore County (UMBC) ScholarWorks@UMBC digital repository on the Maryland Shared Open Access (MD-SOAR) platform.

**Please provide feedback**

Please support the ScholarWorks@UMBC repository by emailing [scholarworks-group@umbc.edu](mailto:scholarworks-group@umbc.edu) and telling us what having access to this work means to you and why it's important to you. Thank you.

# CLIMATE CHANGE IMPACT ON CRITICAL SOURCE AREA IDENTIFICATION IN A MARYLAND WATERSHED

J. Renkenberger, H. Montas, P. T. Leisnham, V. Chanse,  
A. Shirmohammadi, A. Sadeghi, K. Brubaker,  
A. Rockler, T. Hutson, D. Lansing



**ABSTRACT.** *The potential impacts of climate change on critical source areas (CSAs) of surface runoff, sediments, nitrogen, and phosphorus were evaluated in an agricultural watershed of the Chesapeake Bay drainage basin, in the U.S. Northeast climate region. The SWAT model was calibrated for the study watershed and used to establish its baseline response and constituent CSAs under current climate (years 1990 to 2004). The calibrated model was then subjected to weather time series downscaled from the CMIP3 GFDL CM2.1 Atmosphere-Ocean Global Circulation Model (AOGCM) for IPCC SRES scenarios B1 (low emissions), A1B (medium emissions), and A2 (high emissions) to predict the watershed's response to climate change and identify how constituent CSAs may change under future climate (years 2046 to 2064 and 2081 to 2100). The utility of targeting best management practices (BMPs) to CSAs was assessed by computing advantage ratios that relate the fraction of watershed-generated constituents that emanate from CSAs to the fraction of watershed area occupied by these CSAs. Results indicated that, under current conditions, CSAs occupying 11% to 21% of the watershed area contribute 31% to 45% of constituents, corresponding to advantage ratios of 1.5:1 for runoff control and approximately 3:1 for other constituents. Under climate change scenario B1, constituent yields were predicted to increase by factors of 1.5 to 1.8 at the watershed outlet, from an increase in annual rainfall of 25% predicted by the AOGCM, over current conditions. Under scenarios A1B and A2, constituent yields were predicted to increase by factors of 1.8 to 2.3 over current conditions, from an increase of 30% in annual rainfall. The area of runoff CSAs was predicted to more than triple with climate change, leading to negligible advantage of targeting runoff control BMPs to CSAs under future climate. The areas of sediment, nitrogen, and phosphorus CSAs were predicted to increase by factors of 2 to 3 with climate change, causing BMP-targeting advantage ratios to decrease from approximately 3:1 (baseline) to 2:1 (future). While advantage ratios for suspended and dissolved constituents remain favorable, even under future climate, the much larger area predicted to be covered by CSAs (2 to 3 times current values) suggests that stakeholder involvement and community-oriented participatory approaches will be increasingly important for achieving Chesapeake Bay TMDLs with climate change.*

**Keywords.** *Climate change, Critical source areas, Hotspots, Nonpoint-source pollution, NPS, SWAT model, Water quality, Watershed hydrology.*

---

Submitted for review in December 2015 as manuscript number NRES 11677; approved for publication as part of the Climate Change collection by the Natural Resources & Environmental Systems Community of ASABE in September 2016.

The authors are **Jaison Renkenberger, ASABE Member**, Graduate Student, Department of Civil and Environmental Engineering, **Hubert Montas, ASABE Member**, Associate Professor, Fischell Department of Bioengineering, **Paul T. Leisnham, ASABE Member**, Associate Professor, Department of Environmental Science and Technology, **Victoria Chanse**, Associate Professor, Department of Plant Science and Landscape Architecture, and **Adel Shirmohammadi, ASABE Fellow**, Professor, College of Agriculture and Natural Resources, University of Maryland, College Park, Maryland; **Ali Sadeghi, ASABE Member**, Soil Physicist, USDA-ARS Hydrology and Remote Sensing Laboratory, Beltsville, Maryland; **Kaye Brubaker**, Associate Professor, Department of Civil and Environmental Engineering, University of Maryland, College Park, Maryland; **Amanda Rockler**, Watershed Restoration Specialist, Sea Grant Extension, University of Maryland, Derwood, Maryland; **Thomas Hutson**, Senior Agent, University of Maryland Extension - Talbot County, Easton, Maryland; **David Lansing**, Assistant Professor, Department of Geography and Environmental Systems, University of Maryland, Baltimore, Maryland. **Corresponding author:** Hubert Montas, 1453 ANS, University of Maryland, College Park, MD 20742; phone: 301-405-1196; e-mail: montas@umd.edu.

The Chesapeake Bay is the largest and most productive estuarine ecosystem in the U.S. but suffers from substantial water quality degradation (Chesapeake Bay Program, 2012). To help improve Chesapeake Bay water quality, President Obama signed Executive Order 13508, established under the authority of the federal Clean Water Act (CWA) of 1972 (White House, 2009), which led the EPA to develop total maximum daily loads (TMDLs) for total suspended sediment (TSS), total nitrogen (TN), and total phosphorus (TP) for watersheds that drain into the bay (Garvin and Enck, 2010). Agricultural areas, on Maryland's eastern shore portion of the Chesapeake Bay basin, have been identified as a potentially important source of suspended solids and nutrients entering the bay and possibly contributing to eutrophication of the bay's ecosystem (Mueller and Helsel, 2013). Over the past three decades, significant efforts have reduced point-source pollution loadings of sediments and nutrients entering the bay (e.g., wastewater treatment plants, factory or industry outfalls), but nonpoint-source pollution (NPS) has remained challenging to

manage, due to the source of pollution and the size and spatial heterogeneity of the bay's drainage basin. NPS pollution is best tackled by applying best management practices (BMPs) over the landscape (Ritter and Shirmohammadi, 2001). However, land area, time, and monetary resources are limited. For local, county, and state governments to make efficient and effective resource allocations, they need to know where especially vulnerable watershed areas are so that they can focus their BMP adoption and implementation efforts there.

To minimize land area, time, and monetary resources, BMP adoption and implementation efforts can be guided by the identification of vulnerable watershed areas. Vulnerable watershed areas are zones that export target pollutants at rates significantly higher than others, within a given watershed, and are often termed critical source areas (CSAs), or hotspots. Targeting CSAs for BMP implementation is thought to be more advantageous than random placement of BMPs. As a result, various strategies for identifying such areas have been explored in many research studies (Chen et al., 2014; Chu et al., 2004; Huaifeng et al., 2010; Huang et al., 2015; Niraula et al., 2013; Sexton et al., 2010; Shang et al., 2012; White et al., 2009; Winchell et al., 2014). These strategies include the subwatershed load approach (SLA), river/reach load approach (RLA), river/reach concentration approach (RCA), subwatershed load per area approach (SLAA), and HRU load approach (HRULA), with the choice of method typically selected based on scope, purpose, target pollutants, and tools used in the study (Chen et al., 2014). The use of spatially distributed, physically based hydrologic models, in conjunction with geographic information systems (GIS), is currently the preferred approach for CSA identification, but simpler indices and loading functions are still applied where advanced tools are unavailable or training is missing (Niraula et al., 2013).

By the end of the century, the ongoing process of climate change is expected to have caused annual precipitation and storm intensity to undergo substantial increases in the U.S. northeast climate region, where the Chesapeake Bay drainage basin is located (Melillo et al., 2014). Recent studies in other U.S. regions, where precipitation increases are expected to be of lower magnitude, have shown that increases in streamflow, sediment yield, and nitrogen or phosphorus exports of up to 2.5 times their values under current climate are possible with climate change, depending on geographical location and watershed characteristics (Bosch et al., 2014; Van Liew et al., 2012; Woznicki et al., 2011). As a result, one may expect that controlling CSAs identified under current climate in the Chesapeake Bay watershed may no longer be sufficient to control NPS pollution with future climate change. Stated differently, permanent changes in weather may make TMDL attainment more difficult if climate change impacts the placement and characterization of CSAs. Climate models predict variations in rainfall that may cause such CSAs to expand spatially, and this could lead to costly re-planning and or re-design in an effort to maintain TMDL targets for an already managed watershed. The potential extent to which the characteristics of Chesapeake Bay CSAs may vary in response to future climate change is currently unknown.

The objective of this study is to capture and understand what impacts climate change may have on CSAs for Chesapeake Bay watersheds in the U.S. northeast climate region of the Atlantic Coastal Plain physiographic region. The approach used was first to calibrate a hydrologic and water quality model for a representative study watershed under current climate, and then to apply this model to simulate a watershed's response under selected climate change scenarios. The next four sections of this article describe the study watershed, the materials used for the investigation, the methods, and the results.

## STUDY AREA AND STUDY PERIOD

This study is focused on the Greensboro watershed (fig. 1), a 298 km<sup>2</sup> subwatershed of the upper Choptank River (USGS HUC 02060005) located near the town of Goldsboro, Maryland, and extending over part of Caroline County, Maryland, and Kent County, Delaware, on the Delmarva Peninsula. This is one of two gauged watersheds in the Choptank basin and has the most complete dataset. The watershed receives an average of 1070 mm of rainfall annually and is typical of mixed land use watersheds in the Atlantic Lower Coastal Plain, with row crops and hay occupying 39% and 10% of its land area, respectively (cf. data sources in table 2). Other land uses include forested wetlands (23%), deciduous forests (18%), mixed or evergreen forests (2%), and residential or urban land (6%). The Greensboro watershed is relatively flat, with slopes below 1% covering 53% of its area. The distribution of its hydrologic soil groups (HSGs) consists of: A (4%), B (26%), C (50%), and D (20%). The large fractions of B and C HSGs are expected, as the Coastal Plain region is composed of unconsolidated sand, silt, and clay sediments (MGS, 2015). USGS gauging station 01491000, located at the watershed's outlet (38° 59' 49.9" N, 75° 47' 8.9" W), provides continuous monitoring of streamflow along with water quality data from intermittent (approximately monthly) grab samples. Based on these data, a study period spanning the 15 years beginning on 1 January 1990 and ending on 31 December 2004 was selected to represent the watershed's response baseline in this study.

## MATERIALS

Four groups of materials were used in this study: (1) GIS and modeling software, (2) spatial data, (3) baseline time series, and (4) climate change time series. The GIS and modeling software were used throughout the study to develop and calibrate the watershed model, analyze outputs under selected climate regimes, and produce maps of the results. The baseline spatial data and time series were used to develop and calibrate the watershed model and identify baseline CSAs. The climate change time series were used to characterize the watershed's response to climate change and assess the impacts of future climate on CSAs.

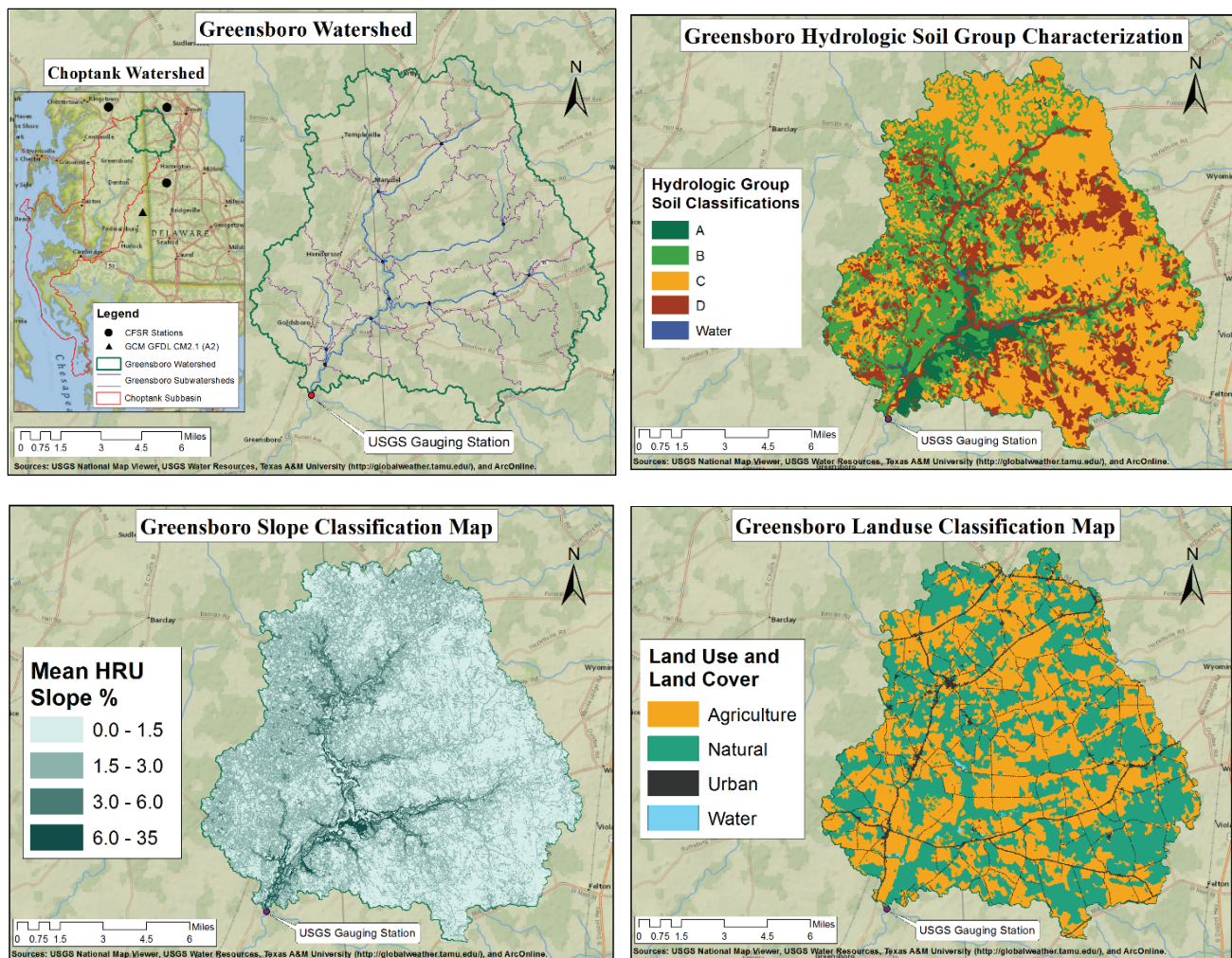


**Figure 1.** Location and weather stations (top left) and spatial characteristics of the study watershed (sources: USGS, NRCS, and USDA databases listed in table 2).

### GIS AND MODELING SOFTWARE

The key software products used in this study are listed in table 1. The primary program used is the Soil and Water Assessment Tool (SWAT). It is a spatially distributed, basin-scale, continuous time, hydrologic and water quality model (Arnold et al., 1993). Forced by observed or predicted weather data, this model has the ability to predict changes in nutrient, sediment, and agri-chemical yields at the watershed outlet and over land elements that result from management actions (Arnold et al., 1993; Gassman et al., 2007). SWAT bases its calculations of runoff and constituent generation, within a watershed, on hydrologic response units (HRUs), which are small land areas representing unique combinations of soil, topography, and land use. Constituents generated by

HRUs are pooled within an individual subwatershed and routed through tributaries to the watershed outlet.

The primary support software for SWAT includes the SWAT Calibration and Uncertainty Programs (SWAT-CUP), a semi-automated calibration tool (Abbaspour et al., 2004; Abbaspour, 2013; Yang et al., 2008). Other support programs include SWAT Check, SWAT Baseflow (BFlow) (Arnold and Allen, 1999; Arnold et al., 1995), and the Web-based Hydrograph Analysis Tool (WHAT) (Lim et al., 2005), which support model input verification, baseflow extraction, and separation of hydrographs produced by SWAT, respectively. These programs are open source and freely available, except for ArcGIS, which was developed by Environmental Systems Research Institute (ESRI Inc.)

**Table 1. Software used in this study.**

Software	Purpose	Source
SWAT	Model development	Texas A&M University ( <a href="http://swat.tamu.edu/software/swat-executables/">http://swat.tamu.edu/software/swat-executables/</a> )
ArcSWAT	Model development	Texas A&M University ( <a href="http://swat.tamu.edu/software/arcswat/">http://swat.tamu.edu/software/arcswat/</a> )
ArcGIS	Spatial analysis	ESRI ( <a href="http://www.esri.com/software/arcgis">http://www.esri.com/software/arcgis</a> )
SWAT Check	Model analysis	Texas A&M University ( <a href="http://swat.tamu.edu/software/swat-check/">http://swat.tamu.edu/software/swat-check/</a> )
SWAT-CUP	Model calibration	Neprash Technology ( <a href="http://www.neprashtechnology.ca/Downloads.aspx">http://www.neprashtechnology.ca/Downloads.aspx</a> )
SWAT BFlow	Model calibration	Environmental Systems, Inc. ( <a href="http://www.envsys.co.kr/~swatbflow/USGS_GOOGLE/display_GoogleMap_for_SWAT_BFlow.cgi?state_name=maryland">http://www.envsys.co.kr/~swatbflow/USGS_GOOGLE/display_GoogleMap_for_SWAT_BFlow.cgi?state_name=maryland</a> )
WHAT	Model calibration	Purdue University College of Engineering ( <a href="https://engineering.purdue.edu/~what/">https://engineering.purdue.edu/~what/</a> )

and is proprietary. They can be run independently of each other, except for ArcSWAT, which is a plug-in for ESRI's ArcGIS.

## SPATIAL DATA

Spatial data on topography, land use, and soils were obtained for the study area from publically available online databases of the USGS, USDA, and USDOJ (NLCD). These data are listed in table 2 along with their characteristics (e.g., year, scale, resolution) and specific source. The maps of the study watershed presented in figure 1 and related statistics on the distribution of land uses, soils, and slopes were produced using this dataset and provide further illustration of its characteristics.

## BASELINE TIME SERIES

The sources and characteristics of time series data used for the baseline period of the study (1990-2004) are listed in table 3. Data for stream discharge (SurQ), total suspended solids (TSS), total nitrogen (TN), and total phosphorus (TP) at the watershed outlet were obtained from the USGS National Water Information System (NWIS) for USGS gauging station 01491000. Weather data were obtained from the NOAA National Weather Service (NWS) National Center for Environmental Prediction (NCEP) Climate Forecast System Reanalysis (CFSR) database, as provided by Texas A&M's (TAMU) Global Weather Data for SWAT website. Data from three weather stations that surround the watershed were used to add spatial heterogeneity in rainfall distribution over the relatively large study area.

## CLIMATE CHANGE TIME SERIES

The climate change time series used in this study are derived from predictions of the Geophysical Fluid Dynamics Laboratory Coupled Model Version 2.1 (GFDL CM2.1) Atmosphere-Ocean General Circulation Model (AOGCM) developed by NOAA (table 4). The model predicts the global changes in temperature, wind, and precipitation that are expected to result from changes in atmospheric CO<sub>2</sub> levels (Nakicenovic and Swart, 2000). The global CO<sub>2</sub> levels that drive the AOGCM are averages of predictions by two carbon cycle models adopted by the Intergovernmental Panel on Climate Change (IPCC): ISAM (Integrated Science Assessment Model; Kheshgi and Jain, 2003) and BERN (Joos et al., 2001). Predictions of the GFDL CM2.1 AOGCM are part of the CMIP3 (Coupled Model Intercomparison Project Phase 3) archived by the Program for Climate Model Diagnosis and Intercomparison (PCMDI) at Lawrence Livermore National Laboratory (LLNL) for the United Nations World Meteorological Organization's (UNWMO) World Climate Research Programme's (WCRP) Working Group on Coupled Modelling (WGCM). This AOGCM was selected for its low root mean square error relative to temperature and precipitation observations (Knutti et al., 2013) and from results of Jha et al. (2006) that suggest it may be more accurate than other models for U.S. conditions.

The use of a single AOGCM is a limitation in the scope of the present study. Each one of the models in the CMIP3 database is expected to produce slightly different predictions of future climate conditions. Given its accuracy at predicting past climate, the selected AOGCM is also expected to be accurate in its future predictions, but such accuracy cannot be guaran-

**Table 2. Spatial data used in this study.**

Data Type	Characteristics	Source
Topography and DEM	USGS NED 2006 10 m DEM	USGS NED ( <a href="http://ned.usgs.gov">http://ned.usgs.gov</a> and <a href="http://datagateway.nrcs.usda.gov/">http://datagateway.nrcs.usda.gov/</a> )
Land use and land cover	NLCD 2006 30 m shapefile	USDA-NRCS National Geospatial Center of Excellence ( <a href="http://datagateway.nrcs.usda.gov/">http://datagateway.nrcs.usda.gov/</a> )
Soils	SSURGO 2012 1:24,000 shapefile	USDA-NRCS ( <a href="http://datagateway.nrcs.usda.gov/">http://datagateway.nrcs.usda.gov/</a> )

**Table 3. Baseline time series data used in this study.**

Data Type	Characteristics	Source
Discharge (SurQ)	USGS Code: 00060 Points: 4383 daily average (m <sup>3</sup> s <sup>-1</sup> )	USGS National Water Information System ( <a href="http://waterdata.usgs.gov/usa/nwis/uv?01491000">http://waterdata.usgs.gov/usa/nwis/uv?01491000</a> )
Total suspended sediment (TSS) <sup>[a]</sup>	USGS Code: 80155 (tons d <sup>-1</sup> ) Points: 197 grab samples	USGS ( <a href="http://waterdata.usgs.gov/usa/nwis/uv?01491000">http://waterdata.usgs.gov/usa/nwis/uv?01491000</a> )
Total nitrogen (TN) <sup>[a]</sup>	USGS Code: 00600 unfiltered <sup>[b]</sup> (mg L <sup>-1</sup> ) Points: 224 grab samples	USGS ( <a href="http://waterdata.usgs.gov/usa/nwis/uv?01491000">http://waterdata.usgs.gov/usa/nwis/uv?01491000</a> )
Total phosphorus (TP) <sup>[a]</sup>	USGS Code: 00665 unfiltered <sup>[b]</sup> (mg L <sup>-1</sup> ) Points: 217 grab samples	USGS ( <a href="http://waterdata.usgs.gov/usa/nwis/uv?01491000">http://waterdata.usgs.gov/usa/nwis/uv?01491000</a> )
Baseline weather	Three stations: daily rainfall, temperature, RH, solar radiation, and wind speed were used.	TAMU NOAA NCDC Reanalysis product ( <a href="http://globalweather.tamu.edu/">http://globalweather.tamu.edu/</a> )

<sup>[a]</sup> Sediment and nutrient data are grab samples taken intermittently (approximately monthly) during the study period.

<sup>[b]</sup> The unfiltered specification indicates that inorganic and organic particles were not filtered.

**Table 4. Climate change time series data used in this study.**

Source Model	Data Characteristics	Source
GFDL CM2.1 (unaltered)	CMIP3 (B1, A1B, and A2) stations: 1 Modeled temperature (°C) and precipitation (mm) Mid-century points (all SRES): 6940 End-century points (all SRES): 7280	NOAA Geophysical Fluid Dynamics Laboratory ( <a href="http://globalweather.tamu.edu/cmip">http://globalweather.tamu.edu/cmip</a> )
BERN and ISAM (averaged)	Carbon dioxide concentration projections Present day: 370 ppmv SRES B1: 484 ppmv (mid) and 540 ppmv (end) SRES A1B: 527 ppmv (mid) and 678 ppmv (end) SRES A2: 529 ppmv (mid) and 766 ppmv (end)	NOAA/IPCC ( <a href="http://www.ipcc-data.org/observ/ddc_co2.html">http://www.ipcc-data.org/observ/ddc_co2.html</a> )

teed. The results of the present study will have to be interpreted within this context, where there is uncertainty in future climate and a single model of this future is considered. The choice of using a single AOGCM was made at the start of this study, when the extent to which climate change might affect CSAs was not known, and at least one AOGCM was needed to quantify this potential effect. Future studies are expected to benefit by considering multiple AOGCMs and comparing how CSAs may change over a range of possible futures. These analyses may be performed within the context of hydrologic uncertainty propagation techniques, such as Latin hypercube sampling (LHS) or modified first-order methods (MFORM) (Sohrabi et al., 2003; Sexton et al., 2011).

This study uses a bias-corrected downscaled version of the global GFDL CM2.1 predictions, developed for high-resolution hydrologic modeling by a collaborative effort of the World Bank, the Nature Conservancy, Climate Central, and Santa Clara University (Girvetz et al., 2013; Maurer et al., 2014; Meehl et al., 2007). The downscaled data were obtained in SWAT format from the dedicated server at TAMU (Climate Change Data for SWAT (CMIP3)) for socio-economic development scenarios of the IPCC Special Report on Emission Scenarios (SRES; Nakicenovic and Swart, 2000) that lead to low, medium, and high future levels of atmospheric CO<sub>2</sub>, scenarios B1, A1B, and A2, respectively (table 4). The B1 scenario is characterized by a world that tends toward a service-based economy and resource efficiency. The A1B scenario reflects a balance between fossil and non-fossil fuel sources, in combination with rapid economic and technological growth worldwide. The A2 scenario is one in which economies and social boundaries remain heterogeneous into the future, and economic and technological growth are slower than for B1 and A1B. Downscaled weather predictions for the study watershed, under these three scenarios, were obtained for two future time periods: mid-century (2046-2064) and end-century (2081-2100).

The bias correction and downscaling approaches used to produce weather time series for hydrologic response modeling under climate change can have an impact on the results of the analysis (Chen et al., 2011; Teutschbein and Seibert, 2012). The method used in the present study is daily bias-corrected spatial disaggregation downscaling, which relies on a grid of 0.5° of latitude and longitude, or cells that are approximately 50 km on a side (Givertz et al., 2013). The size of these downscaling cells was judged to be adequate for the purpose of this study, where agricultural land use and flat topography dominate the area surrounding the study watershed. The accuracy of the bias correction and downscaling were further verified by comparing AOGCM time series to CFSR rainfall data for the study watershed, NCDC data for the Snow Hill station (100 km south of the study watershed, within the same landscape), and NCDC data for the Baltimore-Washington International Airport (BWI) station (100 km west of the study watershed, near urban landscapes). These daily rainfall data were processed through a ten-year moving average to remove daily fluctuations and focus on trends. This analysis demonstrated that the bias-corrected and downscaled GFDL CM2.1 was accurate at predicting past rainfall over the agricultural landscape of the study area and at predicting how it differs from that at BWI.

## METHODS

The work performed to achieve the objectives of this study was separated into four steps: (1) model calibration for the study watershed under current climate, (2) identification of CSAs under current conditions, (3) evaluation of the study watershed's response to climate change, and (4) identification of CSAs under future climate.

### MODEL SETUP AND CALIBRATION

Primary SWAT input data, including topography, land use, and soil characteristics for the study watershed, as well as weather data for the study period, were obtained from the previously listed sources (tables 2 through 4). Spatial data were entered into ArcGIS, and the ArcSWAT plug-in was used to combine them with time series data to produce SWAT input files. The process entailed identification of the watershed boundary and definition of an effective set of outlet-connected tributaries and corresponding subwatersheds based on area topography. This was followed by intersection of spatial data layers to identify and characterize HRUs within each subwatershed. Slope and land use thresholds were set to zero (0% or zero land area) during this process to prevent elimination of infrequent HRUs that may correspond to those unusual combinations of characteristics that lead an HRU to be a hotspot, and to support later map production activities (Wang et al., 2106; Wang, 2015; White et al., 2009). The SWAT model was run with the resulting input files, and the output was evaluated with the accounting and analysis tools listed in table 1.

Model outputs and USGS gauging data were input into the SWAT-CUP software to perform model calibration using the Sequential Uncertainty Fitting Ver. 2 (SUFI-2) method (Abbaspour et al., 2004). Calibration with SUFI-2 involved a nine-step process that ultimately resulted in a fitted parameter range with suggested single values for best fit parameters. It was performed stepwise by constituent, starting with hydrology, then sediment, and finally nutrients, as suggested in the literature (Arnold et al., 2012). The number of simulations per iteration was generally set at 500, and iterations continued until goodness-of-fit statistics stopped improving. However, adjustments were made for the optimum use of time and computational resources because, depending on the number of parameters, a single simulation could take from 10 to 20 min. The selection of parameters for the calibration process was based on sensitivity analyses presented in prior literature on SWAT (Sexton et al., 2011; Wang, 2015). Hydrograph and baseflow analysis tools (WHAT and SWAT Bflow) were used for the initial hydrologic calibration to fit a baseflow coefficient (ALPHA\_BF) and experiment with hydrograph separation and weighting to improve hydrologic statistics, respectively. Additional details on the calibration process can be found in Renkenberger (2015).

The calibrated model performance was evaluated with commonly used statistics, including Pearson's correlation coefficient ( $r$ ), Nash-Sutcliffe efficiency (NSE, also known as coefficient of determination,  $R^2$ , equation 3 in Nash and Sutcliffe, 1970), percent bias, and mean square error (MSE). These are defined in equations 1 through 4, respectively:

$$r = \frac{\sum_{i=1}^n (Y_i^{obs} - \bar{Y}^{obs})(Y_i^{sim} - \bar{Y}^{sim})}{\sqrt{\sum_{i=1}^n (Y_i^{obs} - \bar{Y}^{obs})^2 \sum_{j=1}^n (Y_j^{sim} - \bar{Y}^{sim})^2}} \quad (1)$$

$$NSE = 1 - \frac{\sum_{i=1}^n (Y_i^{obs} - Y_i^{sim})^2}{\sum_{i=1}^n (Y_i^{obs} - \bar{Y}^{obs})^2} \quad (2)$$

$$PBIAS = \frac{\sum_{i=1}^n (Y_i^{obs} - Y_i^{sim})}{\sum_{i=1}^n (Y_i^{obs})} \times 100 \quad (3)$$

$$MSE = \frac{1}{n} \sum_{i=1}^n (Y_i^{sim} - Y_i^{obs})^2 \quad (4)$$

where

$Y_i^{obs}$  = observed values at given time step

$Y_i^{sim}$  = simulated values at given time step

$\bar{Y}^{obs}$  = observed mean

$n$  = number of observations.

Hydrology statistics were calculated on daily, monthly, and annual bases by water year (1 October to 30 September). Statistics for sediment, TN, and TP were calculated annually by calendar year (1 January to 31 December). Recommendations and guidelines for use of these statistics in hydrologic and watershed modeling are discussed by Harmel et al. (2014) and Moriasi et al. (2007). Trend lines were computed by regression between predicted and observed annual values of streamflow, sediment, and nutrients to verify that the calibrated model could replicate the range of values observed for these variables over the study period.

#### BASLINE CRITICAL SOURCE AREAS (CSAs)

Outputs from the calibrated SWAT model were used to identify critical source areas (CSAs) under current climate in the study watershed (baseline conditions). Following the nomenclature of Chen et al. (2014), the method used in this study would be classified as an HRU load per unit area (HRULA) approach. The HRULA approach in our study is coupled with a quantile method in which HRUs exporting the highest concentrations of surface runoff (SurQ), sediments (TSS), nitrogen (TN), and phosphorus (TP) are separated from the rest of the watershed area and considered to be hotspots (CSAs). Two levels, or groups, were used to establish CSAs in this study: the top 10% and the top 20% of HRUs. These hotspots were identified by (1) recording the total number of HRUs ( $N_{HRU}$ ) for the Greensboro watershed SWAT model; (2) ranking each HRU by its production of SurQ ( $\text{mm ha}^{-1}$ ), TSS ( $\text{Mg ha}^{-1}$ ), TN ( $\text{kg ha}^{-1}$ ), and TP ( $\text{kg ha}^{-1}$ ); and (3) marking the top 10% ( $0.1 \times N_{HRU}$ ) of each set of ranked HRUs as the 10% level CSAs and the top 20% of each set ( $0.2 \times N_{HRU}$ ) as the 20% level CSAs. Accordingly, four sets of CSAs (one per constituent) were developed for each of the two selected levels (10% and 20% CSAs). The breakpoint HRULA values for each constituent, marking the boundary between CSA and non-CSA HRUs, were recorded at both CSA target levels for later use

in extending the CSA identification process to climate change conditions. The predicted HRULA values for each constituent were retrieved from the SWAT output file (output.hru), and the corresponding SWAT output variables were combined using equations 5, 6, and 7 to produce the total HRULA for each constituent as needed for ranking (Huang et al., 2015):

$$TSS = (\text{SYLD}) \frac{\text{Mg}}{\text{ha}} \quad (5)$$

$$TN = (\text{OrgN} + \text{NSurQ} + \text{NLatQ} + \text{NO3GW}) \frac{\text{kg}}{\text{ha}} \quad (6)$$

$$TP = (\text{OrgP} + \text{SedP} + \text{SolP} + \text{P}_{\text{GW}}) \frac{\text{kg}}{\text{ha}} \quad (7)$$

where

TSS = total suspended sediment

TN = total nitrogen

TP = total phosphorus

OrgN, OrgP = organic nitrogen and organic phosphorus

NSurQ = nitrogen in surface runoff.

The areal coverage of CSAs ( $A$ ) and the contribution of CSAs to the total mass export ( $\text{Mg year}^{-1}$ ) of constituents generated by HRUs ( $E$ ) were tabulated. These values were interpreted in terms of advantage ratios, defined as  $E:A$ , which quantify the magnitude of export reductions that may be achieved by focusing remediation resources to CSAs. For a given constituent and target level, a large  $E:A$  ratio indicates the possibility of obtaining high water quality returns with low resource investment, by targeting BMPs to CSAs.

A common assumption underlying this study's approach to CSA identification is that a model calibrated at the outlet of a watershed can accurately describe the hydrologic processes taking place within the watershed. In other words, the model can be used to accurately interpolate conditions within the watershed, if it accurately describes its outlet response. This assumption is justified by the structure of physically based, spatially distributed models, such as SWAT, where outlet response results from integrating the individual outputs of spatially distributed HRUs, each of which behaves in accordance to the specific land cover, soil, and topography found at its precise location within the watershed. This assumption is implicit and necessary in most contemporary hydrologic work related to CSAs due to the lack of watersheds instrumented for multi-point, continuous time, flow and constituent monitoring and is adopted in this study. Studies on the potential uses of ancillary data, such as biological surveys, to verify within-watershed predictions of distributed hydrologic models may help to decrease our reliance on this assumption in the future and further increase our confidence in the accuracy of this interpolation process where distributed monitoring data are unavailable (Renkenberger et al., 2016).

#### WATERSHED RESPONSE TO CLIMATE CHANGE

The hydrologic and water quality response of the Greensboro watershed to climate change was evaluated by using the calibrated SWAT model to simulate its behavior with time series downscaled from the GFDL CM2.1 AOGCM as

weather input data. Simulations were performed for the three selected climate change scenarios (B1, A1B, and A2) with time series representing predicted weather at mid-century and end-century (six simulations total). The predictions of annual average streamflow, sediment, total nitrogen, and total phosphorus export produced by these simulations were compared, at the watershed outlet, with corresponding results obtained under baseline conditions. These results were used to identify whether export trends were expected to increase or decrease with changing climate in this watershed and the degree to which they would do so. Predicted trends in watershed export were compared to the trends in precipitation predicted by the downscaled climate models (driving force) and to the literature to explain and contextualize the results.

### EFFECTS OF CLIMATE CHANGE ON CSAS

CSAs were identified by using the HRU-based output of SWAT (output.hru) resulting from the simulations of the hydrology and water quality response of the Greensboro watershed to scenarios B1, A1B, and A2 at mid-century and end-century. These climate change CSAs were extracted at the 10% and 20% levels using the same breakpoint HRULA values established for each constituent in the baseline CSA analysis (fixed threshold approach). In other words, all HRUs producing more than the breakpoint HRULA value established at baseline, for each constituent and target level, are considered hotspots in the predicted watershed response to each climate change scenario. The amount of watershed area occupied by CSAs and their export contributions were computed for the three climate change scenarios, at mid-century and end-century, and compared to baseline results to assess the impact of climate change. The trends in CSA area and export with climate change were compared to trends in watershed outlet response to evaluate the degree to which changes in surface and in-stream responses are consistent with one another. Advantage ratios ( $E:A$ ) were computed for

the climate change CSAs and compared to corresponding values obtained under current climate to quantify the degree to which the benefits of a CSA-based BMP targeting approach may be degraded, maintained, or enhanced for each climate change scenario and constituent in the study area. ArcGIS was used to map the CSAs obtained at the 10% and 20% levels for baseline conditions, and for the climate change scenarios that caused them to change the most, to provide a graphic illustration of the expected impact of future climate on hotspots in the study area.

## RESULTS AND DISCUSSION

### MODEL SETUP AND CALIBRATION

The data preparation steps resulted in a representation of the study watershed composed of 23 subbasins and 7705 HRUs, which was then calibrated using the procedure outlined earlier. Discharge predicted at the watershed outlet by the calibrated model is presented in figure 2 along with observed streamflow and precipitation from one of the three stations used in the model. Predicted flows follow observations relatively well at the daily time step but tend to underpredict on days with the largest discharges. Observed and predicted mean discharges for the study period are  $4.7$  and  $4.1 \text{ m}^3 \text{ s}^{-1}$ , respectively, corresponding to 498 and 434 mm of annual streamflow. The largest difference between observed and predicted flows is for the maximum discharge over the study period ( $158.6 \text{ m}^3 \text{ s}^{-1}$  on 17 September 1999), which is predicted at almost a third of that value ( $57.0 \text{ m}^3 \text{ s}^{-1}$ ). The underpredictions of the largest daily flows in this watershed may be caused by a lack of accounting for snow accumulation and melting, underpredicting humidity, surface runoff lag time, and the use of an “irrigation by need” management approach in the model, which likely underestimates actual practices in the area.

Calibration statistics are presented in table 5. Daily streamflow is relatively well predicted by the model, with a correlation coefficient of 0.66 and an NSE of 0.42, indicating

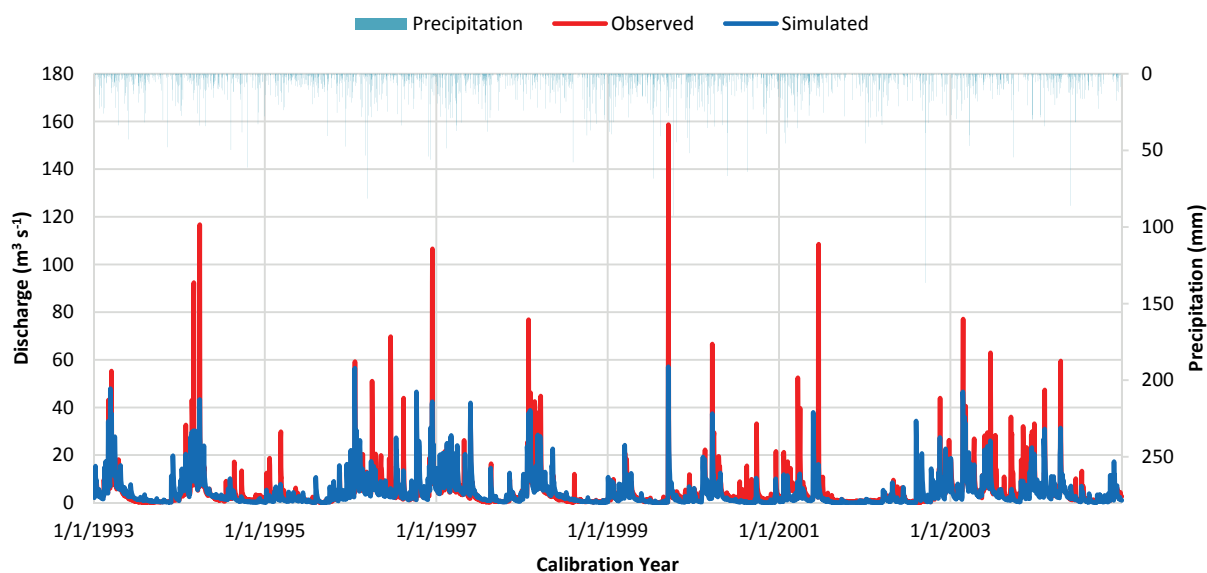


Figure 2. Discharge calibration hydrograph and hyetograph.

**Table 5. Calibration statistics.**

Statistic	Hydrology (SurQ)			Sediment (TSS, annual)	Total Nitrogen (TN, annual)	Total Phosphorus (TP, annual)
	Daily	Monthly	Annual			
r	0.66	0.83	0.80	0.91	0.77	0.91
NSE	0.42	0.66	0.53	0.57	0.47	0.79
Bias (%)	-12.18	-12.28	-9.14	50.12	-13.20	-5.83
MSE	35.52	6.28	1.72	$1.2 \times 10^3 \text{ Mg ha}^{-1}$	$1.7 \times 10^5 \text{ kg ha}^{-1}$	$7.2 \times 10^3 \text{ kg ha}^{-1}$

that the model explains 42% of observed daily flow variability. These statistics improve as the temporal scale is widened to monthly and annual bases, where correlation with observed flows reaches 0.83 and the model explains up to 2/3 of observed flow variations. These statistics are comparable to those reported in other work using the SWAT model in Maryland watersheds (Chu et al., 2004; Sexton et al., 2010, 2011). Calibration of SWAT sediment and nutrient subcomponents on yearly averaged measurements of suspended solids and nutrients results in better correlations (0.77 to 0.91) and Nash-Sutcliffe coefficients (0.47 to 0.79) than for flow, indicating that the overall calibration of the model is adequate for the purpose of simulating the relative response of the watershed to varying hydro-climatic conditions.

Correlations between annual model predictions and observations of discharge, sediment, TN, and TP are shown graphically in figure 3. There is good agreement between observed and predicted discharges on an annual basis, with a regression line slope of 0.9. Sediments are slightly overpredicted, with a slope of 1.2, especially for years with lower sediment loads. TN has a regression line slope of 0.7, indicating some level of underestimation. The trend line in this

case is affected by the data point for 1996, in which nearly twice as much TN was observed as for the second highest nitrogen exporting year. There is good correlation between predicted and observed TP, with a trend line slope of 0.8. In prior studies on other Maryland watersheds, both Chu et al. (2004) and Sexton et al. (2011) noted that 1996 was an unusually wet year. As climate change may generate more years of this type, it is important that the watershed's response is predicted correctly for this case. Calibration results demonstrate that flow, sediment, and TP are accurately predicted for this unusual year, while TN is less accurate. The TN underprediction for 1996 is believed to have resulted from additional nitrogen inputs into this and other Maryland watersheds, in the form of an ammonium-based road deicer, used by county agents during the winter of 1996, which is not accounted for in the model (Sexton et al., 2011). Sexton et al. (2011) also observed that, in Maryland, 1999 contained some particularly wet months with high discharges. The corresponding year is predicted well by the calibrated model, except possibly for a mild underprediction of TP.

It is useful to consider these calibration results in relation to the main objective of this study, which is to identify how

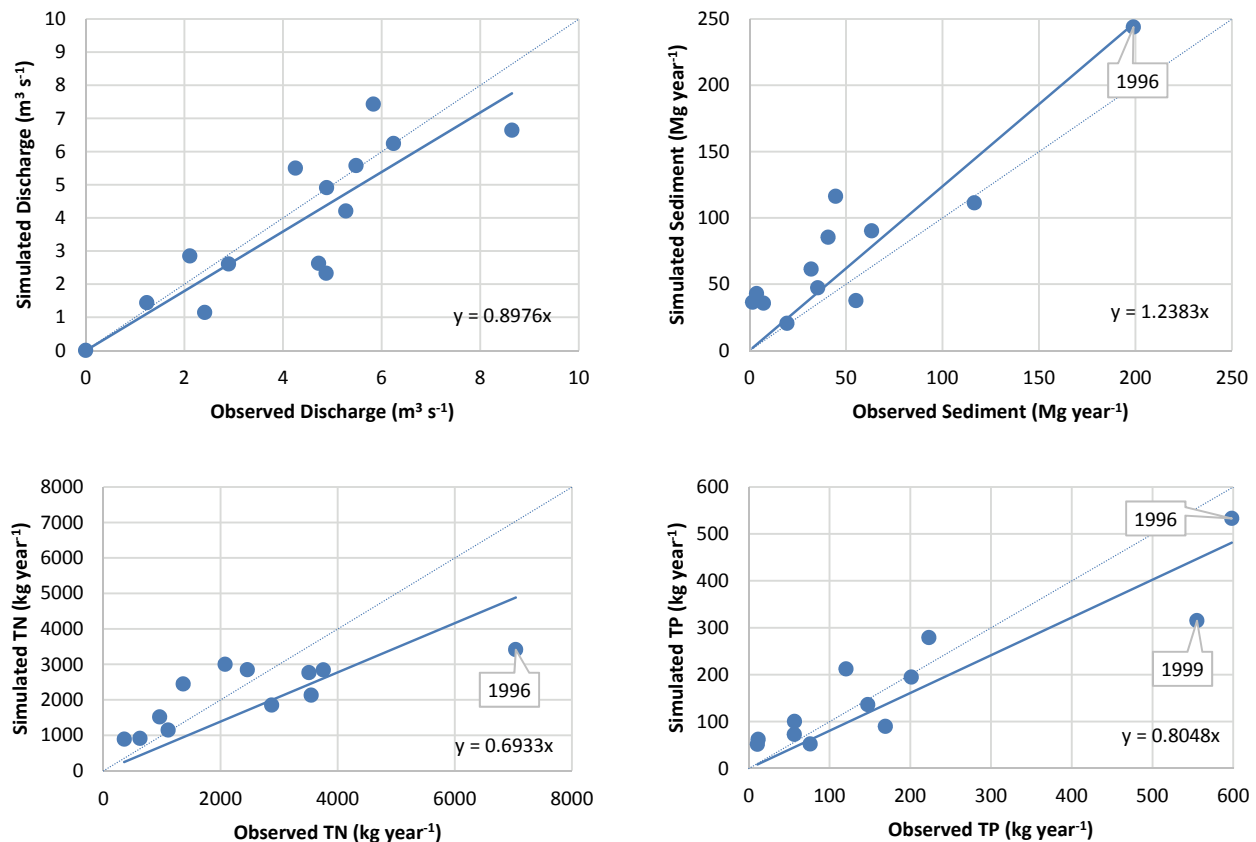


**Figure 3. SWAT annual calibration for Greensboro watershed with trend line ( $y = Kx$ , solid line) and 1:1 line (dotted line).**

climate change may affect CSAs. For this purpose, the relative response of the watershed to increasing or decreasing rainfall produced by the changing climate is most important. In addition, in this study, CSAs are identified based on annual exports of constituents from HRUs. Within this context, the correlations between observed and predicted values, which range between 0.8 and 0.9 on an annual basis, suggest that the calibrated model responds properly to rainfall variations and is suitable for our objective. In addition, the range of the trend lines, from 0.7 to 1.2, suggests relatively mild, and constituent-dependent, underpredictions and overpredictions by the calibrated model. More specifically, if future climate is characterized by increased rainfall, the model is expected to slightly underpredict the corresponding increase in nitrogen and phosphorus exports, and hence underpredict the change in CSAs related to these constituents, and to slightly overpredict the increase in sediment export and the change in sediment CSAs. The calibrated model is not intended to be used for policy-setting in the study watershed, for which higher values of the NSE would be recommended.

#### **BASELINE CRITICAL SOURCE AREAS**

The values of SurQ (surface runoff), TSS, TN, and TP generation above which HRUs are considered to be CSAs at the 10% and 20% levels (breakpoints) are presented in table 6 along with the percentage of watershed area that these HRUs represent and the percentage, by mass, of each constituent that is generated within them. With 7705 HRUs in the watershed, the 10% CSA level consists of the top 771 HRUs in terms of constituent generation, and the 20% level consists of the top 1541 HRUs. With respect to surface runoff, the top 10% and 20% CSAs are those that produce more than 406 and 359 mm, respectively, of runoff annually. The 10% and 20% runoff CSAs occupy 10% and 21% of the watershed area and generate 16% and 31% of the watershed's surface runoff, respectively. These results indicate that, for the Greensboro watershed under current climate, there is a 1.5:1 (or greater) advantage to focusing runoff reduction efforts on CSAs rather than placing related BMPs and control structures at non-CSA locations. A target reduction of 25% of surface runoff may be achieved, for example, by implementing BMPs that are 80% effective over 16% of the watershed area (the top 20% CSAs), whereas a minimum of 31% of the watershed area would need to receive such BMPs if they are placed at non-CSA locations. The smaller implementation area resulting from targeting CSAs is expected to lead to lower financial and social costs while producing the same level of environmental improvement.

Results of CSA identification for sediments and nutrients under current climate are similar to those for surface runoff but with a larger advantage ratio. For sediments, nearly 30% of the generated mass comes from 8% of the watershed area (top 10% CSAs), and nearly 50% comes from 18% of the

area (top 20% CSAs), which corresponds to advantages of 3.4:1 and 2.6:1, respectively, over non-targeted approaches to sediment control. Similarly, 11% of TN is generated over just 3% of the watershed area, and 11% of the area contributes 31% of the generated total, leading to advantage ratios of 3.7:1 and 2.8:1 for the top 10% and 20% of CSAs, respectively. The advantage of targeting BMPs to CSAs is even larger for phosphorus, with ratios of 4.6:1 and 3.0:1 when the top 10% and 20% CSAs are considered, respectively. Overall, these results indicate that under current climate, small land areas within the Greensboro watershed (3% to 21%) contribute substantially to surface runoff (SurQ), TSS, TN, and TP generation (11% to 46%), such that focusing BMP implementation efforts on these hotspots should provide the best ratio of environmental benefits to resource utilization. In other words, targeting CSAs for BMP implementation compared to non-CSA methods would substantially reduce the amount of watershed area that would need to be targeted. This results in the best or most efficient use of finite resources (e.g., subsidies, financial incentives). CSAs obtained at the 20% level are mapped later in this article to compare them graphically to CSAs resulting from climate change.

#### **WATERSHED RESPONSE TO CLIMATE CHANGE**

The predicted response at the outlet of the Greensboro watershed to climate change scenarios B1, A1B, and A2 is compared to its behavior under the current climate baseline in figure 4. At mid-century, there is a substantial increase in annual streamflow, sediments, total nitrogen, and total phosphorus exports for all three climate change scenarios as compared to current climate. This is caused by increases in total rainfall, predicted by the GFDL AOGCM, as shown in table 7. At this time point, the predicted response between scenarios deviates less than at the end of the century. From mid-century to end-century, watershed exports nearly stabilize under scenario B1 but keep increasing under A1B and A2. At end-century, watershed exports are lowest under scenario B1, reaching 681 mm year<sup>-1</sup> of runoff, 0.77 Mg ha<sup>-1</sup> year<sup>-1</sup> of sediments, 17 kg ha<sup>-1</sup> year<sup>-1</sup> of total nitrogen, and 1.2 kg ha<sup>-1</sup> year<sup>-1</sup> of total phosphorus. These represent increases of 56%, 79%, 56%, and 52%, respectively, over the baseline values of 434 mm year<sup>-1</sup> of runoff, 0.43 Mg ha<sup>-1</sup> year<sup>-1</sup> of sediments, 11 kg ha<sup>-1</sup> year<sup>-1</sup> of TN, and 0.78 kg ha<sup>-1</sup> year<sup>-1</sup> of TP. The largest exports are reached under scenario A2 for runoff (826 mm year<sup>-1</sup>), sediments (1.0 Mg ha<sup>-1</sup> year<sup>-1</sup>), and total phosphorus (1.4 kg ha<sup>-1</sup> year<sup>-1</sup>) and represent increases of 90%, 132%, and 80%, respectively, over the baseline. The largest end-century export of total nitrogen occurs under scenario A1B, where 20.5 kg ha<sup>-1</sup> year<sup>-1</sup> of TN flows out of the watershed, which is an 88% increase over the current climate baseline.

The increases in exports predicted under climate change by the calibrated SWAT model for the Greensboro water-

**Table 6. Critical source area breakpoints for baseline conditions at two targeting levels, with corresponding CSA area fraction (*A*) and export contribution (*E*).**

Rank	SurQ			TSS			TN			TP		
	Breakpoint (mm year <sup>-1</sup> )	<i>E</i> (%)	<i>A</i> (%)	Breakpoint (kg ha <sup>-1</sup> year <sup>-1</sup> )	<i>E</i> (%)	<i>A</i> (%)	Breakpoint (kg ha <sup>-1</sup> year <sup>-1</sup> )	<i>E</i> (%)	<i>A</i> (%)	Breakpoint (kg ha <sup>-1</sup> year <sup>-1</sup> )	<i>E</i> (%)	<i>A</i> (%)
Top 10%	>406	16	10	>1030	27	8	>24	11	3	>1.9	23	5
Top 20%	>359	31	21	>730	46	18	>16	31	11	>1.3	39	13

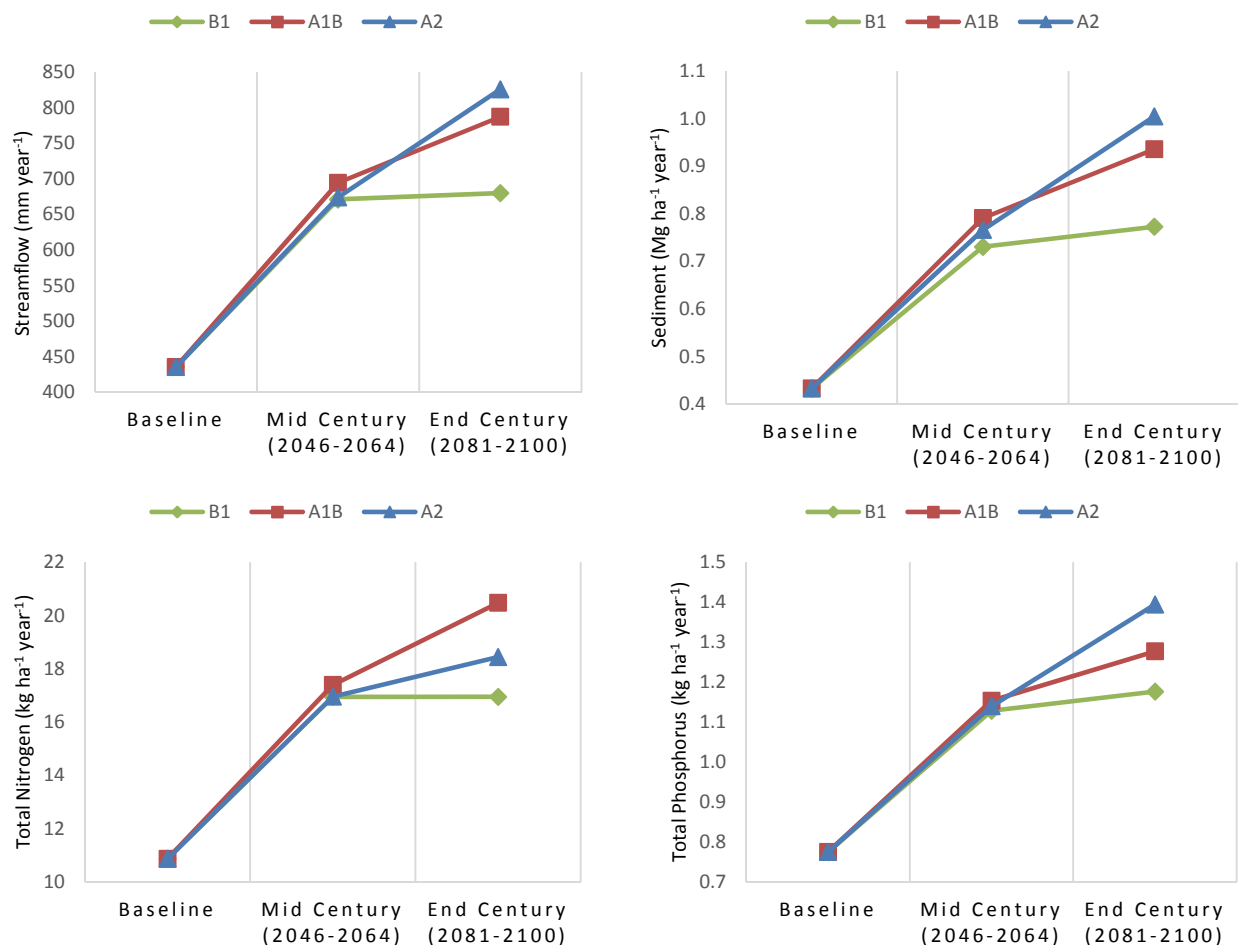


Figure 4. Hydrologic response of the Greensboro watershed (outlet) to climate change scenarios.

Table 7. Percent change in precipitation for SRES B1, A1B, and A2 at end-century above baseline (to compare with the 15-year baseline, only the first 15 years of each scenario's data were used).

Daily Precipitation Event	B1 End	A1B End	A2 End
>80 mm	25%	50%	175%
60 to 80 mm	225%	325%	425%
40 to 60 mm	175%	100%	65%
20 to 40 mm	58%	63%	56%
10 to 20 mm	31%	21%	19%
5 to 10 mm	6%	-19%	-24%
0 to 5 mm	-1%	-33%	-32%
Change in annual precipitation:	25%	30%	29%

shed are consistent with results presented by Woznicki et al. (2011) for an agricultural watershed at the Kansas-Nebraska border. Those authors found the B1, A1B, and A2 scenarios to result in increases in streamflow, sediments, nitrogen, and phosphorus at the outlet of their study watershed. They also found that increases were less significant under scenario B1 than under A1B and A2. For their study area, the climate models predicted increases in annual rainfall of 8% to 15%, which resulted in increases in streamflow, sediment, nitrogen, and phosphorus export of the order of 20% to 50%. In the present study, climate models predict an increase in annual rainfall of 25% to 30% over the Greensboro watershed (table 7); this generates increases of the order of 50% to 90% in predicted streamflow, nitrogen, and phosphorus exports.

In other words, with twice the predicted increase in annual rainfall due to climate change for eastern Maryland, compared to Kansas-Nebraska, the present modeling predicts approximately twice the increase in streamflow and constituent export for the Maryland watershed relative to the increases predicted by Woznicki et al. (2011) for their study watershed. The largest increase in yields predicted here is for sediments (132%) and, while proportionally larger than for the watershed of Woznicki et al. (2011), it is lower than corresponding results for a Nebraska watershed presented by Van Liew et al. (2012), where a 7% increase in rainfall produced an increase in sediment yields of up to 150%.

The differences in rainfall regimes predicted by climate models for the three climate change scenarios (table 7) provide an explanation for the predicted differences in constituent exports. The increase in annual rainfall (over baseline) is smallest for the B1 scenario (25%), which explains why it produces the lowest increases in streamflow and constituents relative to current climate. For the A2 scenario, there is a more substantial increase in large rainfall events (>60 mm) relative to the baseline than in A1B and B1, which leads to more surface runoff, soil detachment, and bound phosphorus transport and helps explain why this scenario produces the largest increases in exports of these constituents. The A1B scenario has the largest increase in annual rainfall (30%), but

the increase is smaller for large events than in A2, and this leads to more infiltration and leaching of nitrogen than in A2, resulting in the higher TN export that is predicted for this scenario (Davis et al., 2009).

The 25% to 30% increase in annual rainfall predicted by the GFDL AOGCM in this study is larger than found in several other studies (Jha et al., 2006; Woznicki et al., 2011; Van Liew et al., 2012; Bosch et al., 2014). One reason for the difference is that the Northeast climate region is expected to undergo a larger increase in rainfall than other U.S. regions (Mellillo et al., 2014). Another reason, as seen in Jha et al. (2006), is that the GFDL CM2.1 AOGCM predicts higher increases in rainfall under future climate than several other CMIP3 Global Climate Models (GCMs), and many studies use an average of these GCMs for their analysis. The multi-model approach has value, given the uncertainty in future climate predictions, but as stated earlier, the GFDL model was chosen for this study because of its higher accuracy, relative to other models, in predicting past climate for North America (Knutti et al., 2013). It is expected that this higher accuracy translates into higher accuracy in prediction of future climate as well. In the eventuality that a multi-model approach proves more accurate, the present results will remain valuable as a possible worst-case scenario for the study area.

#### EFFECTS OF CLIMATE CHANGE ON CSAS

The effects of climate change on the fraction of watershed area occupied by CSAs are presented graphically in figure 5

for the three future climate scenarios. These CSAs correspond to HRUs that produce target constituents at levels that exceed the 20% breakpoint values listed in table 6 established from baseline conditions. For all three climate scenarios, the land area occupied by CSAs is observed to increase markedly from baseline to mid-century, with slightly higher changes in surface runoff and TN CSA areas under A2 than under B1 and A1B. The increase in CSA area mostly continues from mid-century to end-century in A1B and A2, but at a slower rate and with the exception of the TN CSA in A2, which undergoes a decrease in area. For the B1 scenario, the area occupied by CSAs appears relatively constant between mid-century and end-century time points. As expected, these trends in the fraction of watershed area occupied by hotspots follow the increases in streamflow and constituents predicted for the watershed outlet. With increased annual rainfall predicted under climate change, a larger number of HRUs generate runoff and constituents at levels that exceed the breakpoints established under baseline conditions. However, the relative magnitude by which CSA areas increase is larger than that of constituents at the outlet, as will be seen below, leading to a decrease in the advantage gained by targeting BMP implementation to CSAs. Surface runoff is most notable in this respect with end-century CSAs (HRUs generating more than 359 mm year<sup>-1</sup>) that cover 70% to 80% of the watershed area.

Figure 6 presents the annual yields of surface runoff, sediment, total nitrogen, and total phosphorus produced by the

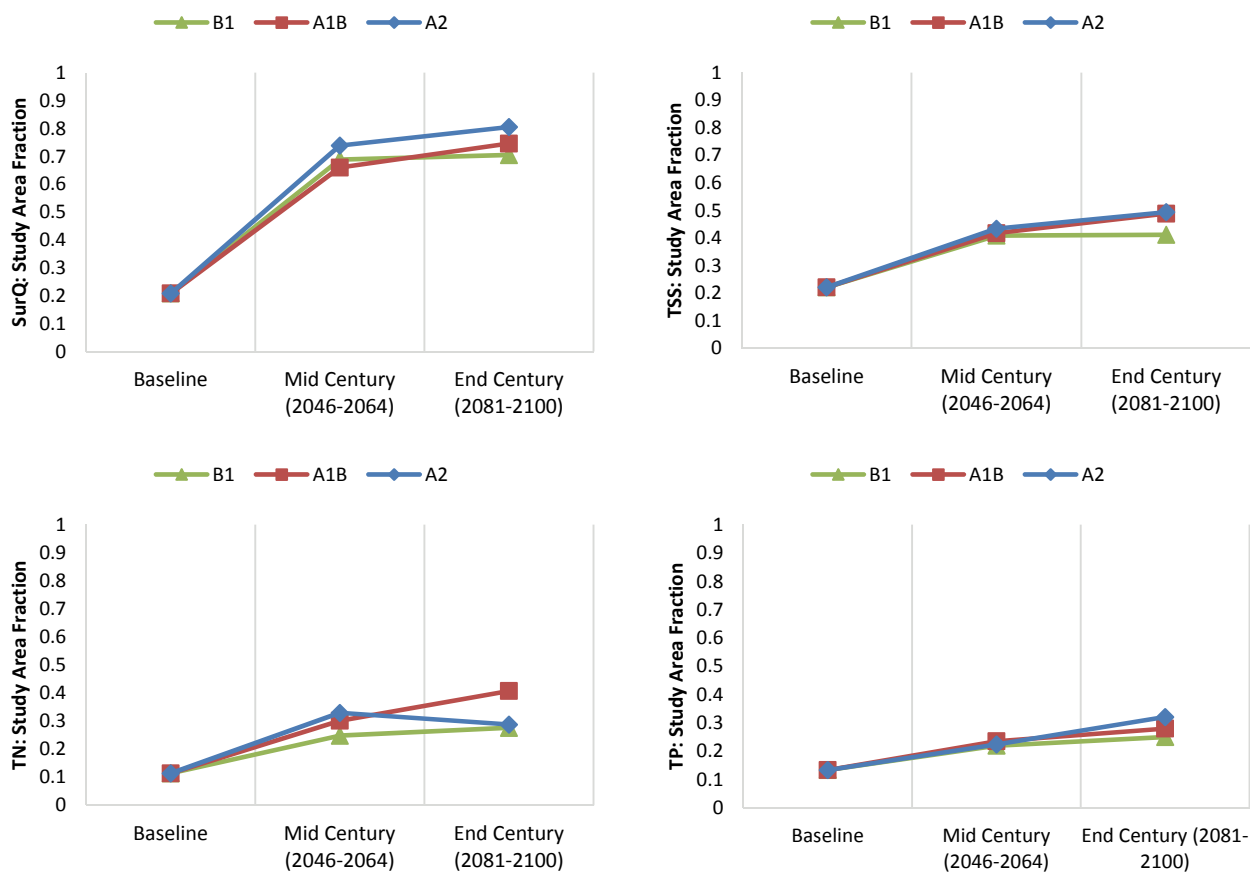


Figure 5. Change in watershed area fraction of CSAs under SRES B1, A1B, and A2 climate scenarios.

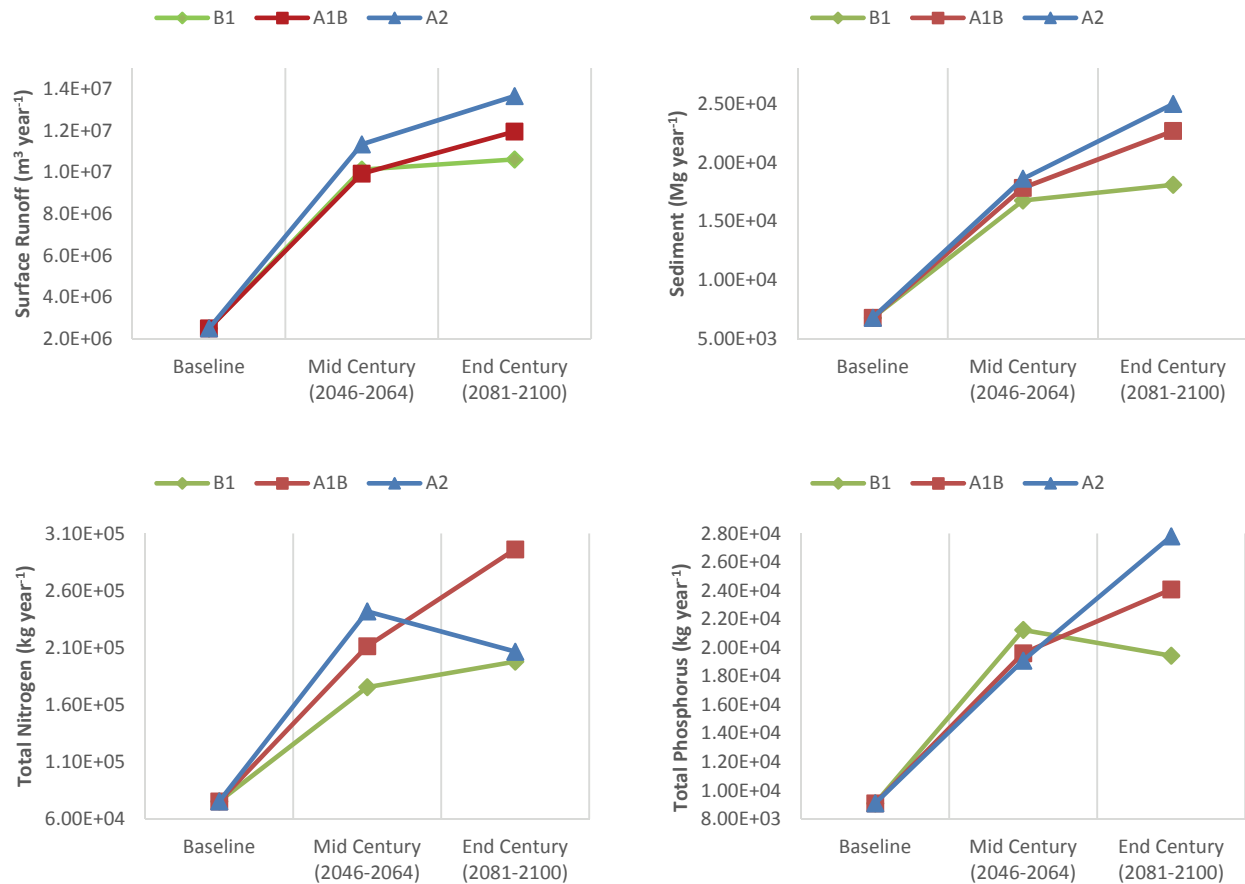


Figure 6. Constituent export from CSAs under SRES B1, A1B, and A2 scenarios.

CSA HRUs at mid-century and end-century for the three climate change scenarios. These curves follow trends similar to those for constituent export at the watershed outlet and for changes in CSA areas. The magnitude by which these quantities increase under future climate is amplified by both the predicted increase in rainfall and the increase in CSA area. For example, under the A2 scenario, the annual amount of sediments generated by CSAs at end-century is predicted to be nearly 5 times the amount generated under baseline conditions because increased rainfall quantity and intensity are producing more sediments on each HRU and, jointly, CSA areas have increased by 2.5 times. Similarly, under A1B at end-century, total nitrogen export is predicted to be more than 4 times larger than under current climate because of increases in lower intensity precipitation (relative to A2) and a greater than 3 times increase in CSA area.

The percentage of watershed area occupied by CSAs and their export contribution relative to the amount of constituents generated by all HRUs in the study watershed are presented in table 8 for the three climate change scenarios (end-

century) and the current climate baseline. For surface runoff, CSAs cover 21% of the watershed under current climate and 70% (B1) to 81% (A2) of the area under climate change. These CSAs contribute 31% of the total surface runoff produced within the watershed in current conditions and 82% (B1) to 89% (A2) with changed climate. The advantage ratio obtained by targeting runoff control BMPs to CSAs drops from 1.5:1 under current climate to between 1.1:1 (A2) and 1.2:1 (B1) with climate change. In this case, the low advantage ratio and large targeted area suggest that, under climate change, a CSA-based approach to surface runoff control will no longer be valuable. Indeed, the present results suggest that surface runoff control measures will be required on all agricultural and urban lands within the study watershed to achieve the same level of reduction attainable under current climate with runoff BMPs covering just 21% of the land.

For sediments, the area of CSAs is predicted to more than double as a result of climate change, from 18% of the watershed area in current climate to between 37% (B1) and 45%

Table 8. Hotspot area fraction (*A*), export contribution (*E*), and advantage ratios (*E:A*) at baseline and at end of century.

Constituent	Baseline			B1			A1B			A2		
	<i>E</i> (%)	<i>A</i> (%)	<i>E:A</i> Ratio	<i>E</i> (%)	<i>A</i> (%)	<i>E:A</i> Ratio	<i>E</i> (%)	<i>A</i> (%)	<i>E:A</i> Ratio	<i>E</i> (%)	<i>A</i> (%)	<i>E:A</i> Ratio
SurQ	31	21	1.5:1	82	70	1.2:1	86	75	1.1:1	89	81	1.1:1
TSS	46	18	2.6:1	75	37	2.0:1	78	45	1.7:1	81	45	1.8:1
TN	31	11	2.8:1	56	28	2.0:1	72	41	1.8:1	57	29	2.0:1
TP	39	13	3.0:1	60	25	2.4:1	63	28	2.3:1	66	32	2.1:1

(A1B, A2). In current climate, the CSAs generate 46% of sediments produced in the basin, and this increases to between 75% (B1) and 81% (A2) under climate change. The advantage of implementing sediment control BMPs on CSAs drops from 2.6:1 in current conditions to between 1.8:1 (A1B) and 2.0:1 (B1) with climate change. These advantage ratios suggest that targeting sediment control BMPs to CSAs will remain a valuable strategy with changing climate in this watershed. However, the 45% of land covered by CSAs in A1B and A2 represents more than 80% of the agricultural and urban land in the basin; therefore, from a practical standpoint (and assuming no sediment production in forests and wetlands), nearly all watershed stakeholders may need to be involved in sediment BMP implementation and maintenance if those more severe climate change scenarios are realized.

The area fraction of CSAs for total nitrogen is predicted to increase from 11% in current conditions to between 28% (B1) and 41% (A1B) with changed climate, and their relative export contributions are predicted to approximately double from 31% currently to between 56% (B1) and 72% (A1B). The corresponding advantage ratios decrease from 2.8:1 currently to between 1.8:1 (A1B) and 2.0:1 (B1), suggesting that CSA-based BMP targeting will remain valuable, especially if the B1 or A2 scenarios are realized. For phosphorus, the predicted increase in CSA area fraction is from 13% currently to between 25% (B1) and 32% (A2) with CSA contributions that increase from 39% of the watershed total presently to between 60% (B1) and 66% (A2). For this constituent, CSA-based targeting of BMPs remains valuable despite a decrease of advantage ratios from 3.0:1 under current climate to between 2.1:1 (A2) and 2.4:1 (B1) with changing climate.

It is interesting to compare the reductions of advantage ratios predicted above to the results obtained under current climate by Wang (2015) for a suburban and an urban watershed in Maryland's Piedmont and Atlantic Coastal Plain physiographic regions. The advantage ratios for the suburban watershed were similar to those obtained for the Greensboro watershed under current climate (approximately 1.5:1, 2.7:1, 2.5:1, and 2.2:1 for SurQ, TSS, TN, and TP, respectively), while those for the urban watershed were similar to those obtained in the present study under climate change (approximately 1.3:1, 1.7:1, 1.6:1, and 2.3:1, respectively). Accordingly, one might consider, at first analysis, that the impact of climate change on the study watershed is to render its pervious areas less effective at buffering the increased amounts of runoff caused by changing rainfall patterns, making it behave in a manner similar to an urban environment, where infiltration capacity is frequently overwhelmed by rainfall (and stormwater sewer systems carry this excess rainfall out of the watershed). With respect to water quality, the present results suggest that, with climate change, a broader segment of the residents of agricultural watersheds will need to participate in BMP implementation, in a manner similar to what is currently needed in urban environments under today's climate. As a consequence, community-oriented approaches to watershed sustainability, targeted at rural audiences, are expected to become increasingly relevant in the northeast U.S. (Leisnham et al., 2013; Chanse et al., 2014).

Maps of CSAs for surface runoff, sediment, and nutrient generation are presented in figure 7 for current climate and for the climate change scenarios that produce the largest increase in CSA area for each constituent (A2 for surface runoff, TSS and TP, and A1B for TN). The red areas in these maps depict HRUs that fall above the 10% CSA breakpoint values in table 6, and the combination of orange and red areas represents CSAs obtained at the 20% breakpoint level. These maps clearly illustrate the substantial increase in CSA area caused by climate change. In the case of runoff, the current climate CSAs are found on a few areas with soils of hydrologic soil groups (HSGs) C and D, in the eastern part of the watershed and near streambeds. Climate change under scenario A2 causes these CSAs to expand to cover most of the watershed, including areas with HSGs A and B. For sediments, the CSAs under current conditions are concentrated on a few high slope areas, in the western half of the watershed; climate change (scenario A2) expands those areas to cover the western half almost entirely, and produces several new CSAs near streams in the eastern subbasin. In the case of total nitrogen, the current climate CSAs consist of numerous small areas with agricultural or urban land use on infiltrable soils (HSGs A and B), mostly in the western half of the watershed; climate change (A1B) causes these areas to grow to include agricultural zones on less infiltrable HSG C soils and a larger proportion of both the western and eastern halves of the basin. For phosphorus, the CSAs under current climate also consist of several small export areas with agricultural land use, but contrary to total nitrogen, these areas are mostly in the eastern half of the watershed, on HSG C and D soils that promote surface runoff production. Climate change scenario A2 expands these CSAs to nearly all watershed areas with poorly infiltrable soil.

The results presented here are to be interpreted in the context of the approach used in this work to define CSAs, which applies a fixed set of thresholds, derived from baseline conditions, to define HRU hotspots under future climate. A consequence of this choice is that the increased annual rainfall predicted to occur under the three predicted scenarios (relative to the baseline) necessarily produced a concomitant increase in the area occupied by hotspots. This increase was not followed with a proportional increase in relative export contributions and therefore led to reduced advantage ratios. An alternative approach would have been to re-rank HRUs (by constituent) at the end of the simulations for each scenario and to consider the top 20% of them as CSAs. The fixed threshold approach was selected for this study so that the impacts of climate change on water quality could be evaluated in relation to today's water quality objectives rather than relative to a baseline that shifts upward as climate change manifests along the selected scenarios. To illustrate the difference between the two approaches, one may consider phosphorus as an example. If the baseline CSAs at the 20% level (HRU breakpoint of 1.3 kg ha<sup>-1</sup> year<sup>-1</sup> from table 6) are targeted today to obtain a 40% decrease in TP export at the watershed outlet from 0.78 to 0.47 kg ha<sup>-1</sup> year<sup>-1</sup>, then this reduction can be achieved, essentially, by placing 100% efficient BMPs on the baseline CSAs (neglecting additional attenuation from in-stream processes). Using a relative targeting approach, at the end-century mark, under the mildest climate change scenario (B1), the objective

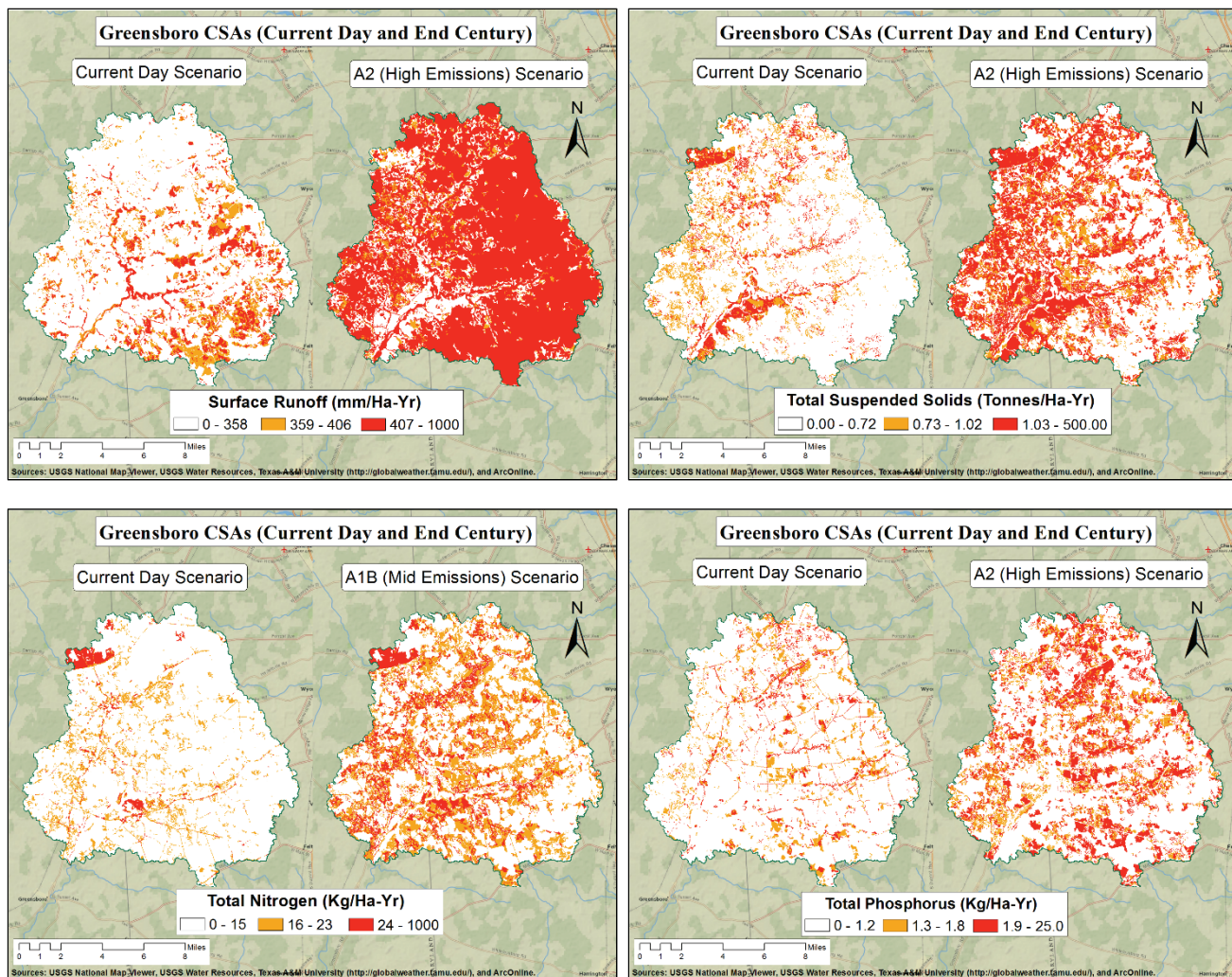


Figure 7. Changes in critical source export area by target pollutant and climate scenarios.

of reducing TP export by 40% at that time would correspond to a reduction from the  $1.2 \text{ kg ha}^{-1} \text{ year}^{-1}$  predicted at end-century to  $0.72 \text{ kg ha}^{-1} \text{ year}^{-1}$ . This target is 1.5 times greater than the target established based on today's hydro-climatic conditions and may not meet the desired water quality standards or the NPS component of a TMDL (i.e., load allocation; Sexton et al., 2011). With the fixed breakpoint approach of the present study, applying 100% efficient BMPs on the TP CSAs identified at end-century for the B1 scenario would lead to the same export level of  $0.47 \text{ kg ha}^{-1} \text{ year}^{-1}$  as is obtained with current climate (again neglecting in-stream processes). Although the equality in this example is fortuitous, it is readily verified that the expected TP exports, with CSAs defined using fixed thresholds and 100% efficient BMPs, under A1B and A2, at end-century, are  $0.51$  and  $0.44 \text{ kg ha}^{-1} \text{ year}^{-1}$ , respectively, both of which are significantly closer to the present day target of  $0.47 \text{ kg ha}^{-1} \text{ year}^{-1}$  of this example than would be obtained with a relative threshold. Similar results are obtained for sediments and nitrogen provided that BMPs are 90% to 100% efficient, and for surface runoff provided that BMPs reduce runoff by 2/3 on the CSAs. The relative threshold approach to CSA identification may become more useful when specific concentrations are used as targets of watershed analysis or if

TMDLs are updated to account for changes in streamflow resulting from climate change, which are to be investigated in future work.

## SUMMARY AND CONCLUSIONS

This study evaluated the potential effects of climate change on the distribution of runoff, sediment, nitrogen, and phosphorus CSAs in an agricultural watershed that flows into the Chesapeake Bay. The bay's location in the U.S. northeast climate region is expected to cause it to receive the largest increases in annual rainfall and storm intensity of the conterminous U.S. Spatial data representing watershed soils, topography, land use, and hydrography were obtained from federal databases. Discharge and concentrations of sediments, nitrogen, and phosphorus in streamflow at the watershed outlet were obtained from the USGS, and weather data were obtained from NOAA for the 15-year calibration period from 1990 to 2004. The spatial and weather data were used to develop input files for the SWAT hydrologic model, which was then calibrated against the outlet data using the SUFI-2 method. The correlation coefficients between the calibrated model and observed values ranged from 0.8 to 0.9

on an annual basis, Nash-Sutcliffe coefficients ranged from 0.5 to 0.8, and regression lines between predicted and observed values had slopes of 0.7 to 1.2. These calibration results are comparable to values from the literature that were considered to range from satisfactory to very good.

CSAs of runoff, sediments, TN, and TP were identified from the output of the calibrated model, representing baseline conditions (current climate). CSAs were determined separately for each constituent at two threshold levels, corresponding to the 10% and 20% of top generating HRUs in the watershed, and their areas and export contributions were computed. The efficiency advantage resulting from targeting BMPs to CSAs (ratio of export contribution to area,  $E:A$ ) were calculated for all constituents and threshold levels. At the 10% threshold, baseline CSAs occupied 3% to 10% of the watershed area and contributed 11% to 27% of constituents. At the 20% level, they occupied 11% to 21% of the area and contributed 31% to 45% of constituents. The advantage ratios under current climate were approximately 1.5:1 for runoff and 3:1 for other constituents (slightly higher at the 10% level and lower at the 20% level, as expected), indicating, for example, that phosphorus exports may be reduced by nearly 40% by placing BMPs on 13% of the watershed area.

The response of the study watershed to climate change was evaluated by simulation, using the calibrated SWAT model, with weather time series downscaled from predictions of the NOAA GFDL CM2.1 AOGCM for mid-century (2046-2064) and end-century (2081-2100) time frames under SRES scenarios B1 (low emissions), A1B (medium emissions), and A2 (high emissions). The increase in annual precipitation predicted by the AOGCM at end-century ranged from 25% (B1) to 30% (A1B and A2) over current climate. In response, streamflow at the watershed outlet was predicted to increase by 56% (B1) to 90% (A2) over current conditions. Sediment yield was predicted to increase by 79% (B1) to 132% (A2), TN by 56% (B1) to 88% (A1B), and TP by 52% (B1) to 80% (A2) over current conditions in response to climate change. Stated differently, a low emissions future (B1) is predicted to produce increases of 50% to 80% in watershed yields over current conditions (a factor of 1.5 to 1.8 times the current yields), while medium or high emissions futures (A1B or A2) produce increases over a higher bracket at 80% to 132% (factors of 1.8 to 2.3 times current yields) in the study area.

CSAs were identified from outputs of calibrated SWAT model simulations of the study watershed's response to climate change using the 20% threshold level of the baseline analysis. For surface runoff, climate change was predicted to cause the area of CSAs to more than triple relative to baseline conditions, from 21% under current climate to between 70% (B1) and 81% (A2) of the watershed area. The contribution of these CSAs to total runoff generation more than doubled, but advantage ratios dropped from 1.5:1 under current climate to approximately 1.1:1 with climate change, suggesting that targeting runoff control BMPs to CSAs will no longer be valuable under future climates. The areas occupied by CSAs for other constituents were predicted to increase by factors of mostly 2 to 3 under climate change, and

their export contribution were predicted to increase by factors near 2, resulting in advantage ratios that decreased from 3:1 in the baseline to approximately 2:1 with climate change. Accordingly, CSA targeting of BMPs for sediment, nitrogen, and phosphorus control is expected to remain valuable with climate change. However, the large predicted increase in watershed area covered by CSAs suggests that a larger number of stakeholders may need to be involved in BMP implementation with climate change (2 to 3 times more than under current conditions). Consequently, community-oriented participatory approaches related to water quality education and to BMP adoption, implementation, and maintenance are expected to become more important in helping to meet the Chesapeake Bay TMDLs, even in rural environments, as climate changes.

The results and conclusions presented here have to be interpreted within the scope of this study, in which a single AOGCM was used. An evaluation of differences in predicted changes in CSAs resulting from the use of alternative AOGCMs would be an interesting study for future research. Additionally, as future rainfall regimes are expected to display a seasonal distribution that differs from that under current climate, it should be interesting to investigate the potential impacts of this seasonal change on CSAs in the study area. Recent analyses by Woznicki and Nejadhashemi (2012) and Mukundan et al. (2013), for example, suggest that seasonal rainfall variations, under future climate, will affect both sediment yields and BMP effectiveness. The results presented herein are not meant for policy-setting in the study area, for which additional calibration steps would be required, and assume that SWAT is an adequate interpolator of within-watershed conditions based on outlet calibration.

## ACKNOWLEDGEMENTS

This project was supported by Competitive Grant No. 2012-51130-20209 from the USDA National Institute of Food and Agriculture.

## REFERENCES

- Abbaspour, K. C. (2013). SWAT-CUP 2012. Vancouver, British Columbia, Canada: Neprash Technology. Retrieved from <http://www.neprashtechnology.ca/Downloads/>
- Abbaspour, K. C., Johnson, C. A., & van Genuchten, M. Th. (2004). Estimating uncertain flow and transport parameters using a sequential uncertainty fitting procedure. *Vadose Zone J.*, 3(4), 1340-1352. <http://dx.doi.org/10.2136/vzj2004.1340>
- Arnold, J. G., & Allen, P. M. (1999). Automated methods for estimating baseflow and ground water recharge from streamflow records. *JAWRA*, 35(2), 411-424. <http://dx.doi.org/10.1111/j.1752-1688.1999.tb03599.x>
- Arnold, J. G., Allen, P. M., & Bernhardt, G. (1993). A comprehensive surface-groundwater flow model. *J. Hydrol.*, 142(1-4), 47-69. [http://dx.doi.org/10.1016/0022-1694\(93\)90004-S](http://dx.doi.org/10.1016/0022-1694(93)90004-S)
- Arnold, J. G., Allen, P. M., Muttiah, R., & Bernhardt, G. (1995). Automated base flow separation and recession analysis techniques. *Ground Water*, 33(6), 1010-1018. <http://dx.doi.org/10.1111/j.1745-6584.1995.tb00046.x>
- Arnold, J. G., Moriasi, D. N., Gassman, P. W., Abbaspour, K. C., White, M. J., Srinivasan, R., ... Jha, M. K. (2012). SWAT: Model use, calibration, and validation. *Trans. ASABE*, 55(4). <http://dx.doi.org/10.13031/2013.42256>

- Bosch, N. S., Evans, M. A., Scavia, D., & Allan, J. D. (2014). Interacting effects of climate change and agricultural BMPs on nutrient runoff entering Lake Erie. *J. Great Lakes Res.*, 40(3), 581-589. <http://dx.doi.org/10.1016/j.jglr.2014.04.011>
- Chanse, V., Leisnham, P., Rockler, A., McCoy, J., Cain, L., Wilson, S., Montas, H., ... Mohamed, A. (2014). A community-based participatory research approach for stormwater management: Implications of differing BMP approaches in two urban watersheds (abstract). In *Proc. EDRA45 New Orleans*. St. Paul, MN: Environmental Design Research Association.
- Chen, J., Brissette, F. P., & Leconte, R. (2011). Uncertainty of downscaling method in quantifying the impact of climate change on hydrology. *J. Hydrol.*, 401(3-4), 190-202. <http://dx.doi.org/10.1016/j.jhydrol.2011.02.020>
- Chen, L., Zhong, Y., Wei, G., Cai, Y., & Shen, Z. (2014). Development of an integrated modeling approach for identifying multilevel nonpoint-source priority management areas at the watershed scale. *Water Resour. Res.*, 50(5), 4095-4109. <http://dx.doi.org/10.1002/2013WR015041>
- Chesapeake Bay Program. (2012). Discover the Chesapeake. Annapolis, MD: Chesapeake Bay Program. Retrieved from <http://www.chesapeakebay.net/discover/bay101/facts>
- Chu, T. W., Shirmohammadi, A., Montas, H., & Sadeghi, A. (2004). Evaluation of the SWAT model's sediment and nutrient components in the Piedmont physiographic region of Maryland. *Trans. ASAE*, 47(5), 1523-1538. <http://dx.doi.org/10.13031/2013.17632>
- Davis, A. P., Hunt, W. F., Traver, R. G., & Clar, M. (2009). Bioretention technology: Overview of current practice and future needs. *J. Environ. Eng.*, 135(3), 109-117. [http://dx.doi.org/10.1061/\(ASCE\)0733-9372\(2009\)135:3\(109\)](http://dx.doi.org/10.1061/(ASCE)0733-9372(2009)135:3(109))
- Garvin, S. M., & Enck, J. A. (2010). Chesapeake Bay TMDL development. Washington, DC: U.S. Environmental Protection Agency. Retrieved from <http://www2.epa.gov/chesapeake-bay-tmdl/chesapeake-bay-tmdl-document>
- Gassman, P. W., Reyes, M. R., Green, C. H., & Arnold, J. G. (2007). The Soil and Water Assessment Tool: Historical development, applications, and future research directions. *Trans. ASABE*, 50(4), 1211-1250. <http://dx.doi.org/10.13031/2013.23637>
- Girvetz, E. H., Maurer, E. P., Duffy, P. B., Ruesch, A., Thrasher, B., & Zganjar, C. (2013). Making climate data relevant to decision making: The important details of spatial and temporal downscaling. Washington, DC: The World Bank. Retrieved from <https://scholarcommons.scu.edu/handle/11123/641>
- Harmel, R. D., Smith, P. K., Migliaccio, K. W., Chaubey, I., Douglas-Mankin, K. R., Benham, B., ... Robson, B. J. (2014). Evaluating, interpreting, and communicating performance of hydrologic/water quality models considering intended use: A review and recommendations. *Environ. Model. Software*, 57, 40-51. <http://dx.doi.org/10.1016/j.envsoft.2014.02.013>
- Huaifeng, G. E., Zuhao, Z., Dayong, Q., Jiguo, Y., & Qiang, C. (2010). Analysis of critical source areas about multi-source nutrient loadings based on SWAT model in Jiyun River basin. *Trans. Hong Kong Inst. Eng.*, 17(2), 14-19. <http://doi.org/10.1080/1023697X.2010.10668191>
- Huang, J. J., Lin, X., Wang, J., & Wang, H. (2015). The precipitation-driven correlation-based mapping method (PCM) for identifying the critical source areas of nonpoint-source pollution. *J. Hydrol.*, 524, 100-110. <http://dx.doi.org/10.1016/j.jhydrol.2015.02.011>
- Jha, M. K., Arnold, J. G., Gassman, P. W., Giorgi, F., & Gu, R. R. (2006). Climate change sensitivity assessment on upper Mississippi River basin streamflows using SWAT. *JAWRA*, 42(4), 997-1016. <http://dx.doi.org/10.1111/j.1752-1688.2006.tb04510.x>
- Joos, F., Prentice, I. C., Sitch, S., Meyer, R., Hooss, G., Plattner, G.-K., ... Hasselmann, K. (2001). Global warming feedbacks on terrestrial carbon uptake under the Intergovernmental Panel on Climate Change (IPCC) emission scenarios. *Global Biogeochem. Cycles*, 15(4), 891-907. <http://dx.doi.org/10.1029/2000GB001375>
- Kheshgi, H. S., & Jain, A. K. (2003). Projecting future climate change: Implications of carbon cycle model intercomparisons. *Global Biogeochem. Cycles*, 17(2), 1047. <http://dx.doi.org/10.1029/2001GB001842>
- Knutti, R., Masson, D., & Gettelman, A. (2013). Climate model genealogy: Generation CMIP5 and how we got there. *Geophys. Res. Lett.*, 40(6), 1194-1199. <http://dx.doi.org/10.1002/grl.50256>
- Leisnham, P., Montas, H., Shirmohammadi, A., Chanse, V., Lansing, D., Rockler, A., ... Wang, Y. (2013). Watershed diagnostics for improved adoption of management practices: Integrating biophysical and social factors across urban and agricultural landscapes. ASABE Paper No. 131668614. St. Joseph, MI: ASABE. <http://dx.doi.org/10.13031/aim.20131668614>
- Lim, K. J., Engel, B. A., Tang, Z., Choi, J., Kim, K.-S., Muthukrishnan, S., & Tripathy, D. (2005). Automated web GIS based hydrograph analysis tool, WHAT. *JAWRA*, 41(6), 1407-1416. <http://dx.doi.org/10.1111/j.1752-1688.2005.tb03808.x>
- Maryland Geological Survey. (2015). Maryland geology. Baltimore, MD: Maryland Geological Survey. Retrieved from <http://www.mgs.md.gov/geology/>
- Maurer, E. P., Brekke, L., Pruitt, T., Thrasher, B., Long, J., Duffy, P., ... Arnold, J. (2014). An enhanced archive facilitating climate impacts and adaptation analysis. *Bull. American Meteorol. Soc.*, 95(7), 1011-1019. <http://dx.doi.org/10.1175/BAMS-D-13-00126.1>
- Meehl, G. A., Covey, C., Taylor, K. E., Delworth, T., Stouffer, R. J., Latif, M., ... Mitchell, J. F. (2007). The WCRP CMIP3 multimodel dataset: A new era in climate change research. *Bull. American Meteorol. Soc.*, 88(9), 1383-1394. <http://dx.doi.org/10.1175/BAMS-88-9-1383>
- Melillo, J. M., Richmond, T. C., & Yohe, G. W. (2014). Climate change impacts in the United States: The third national climate assessment. Washington, DC: U.S. Global Change Research Program.
- Moriassi, D. N., Arnold, J. G., Van Liew, M. W., Bingner, R. L., Harmel, R. D., & Veith, T. L. (2007). Model evaluation guidelines for systematic quantification of accuracy in watershed simulations. *Trans. ASABE*, 50(3), 885-900. <http://dx.doi.org/10.13031/2013.23153>
- Mueller, D., & Helsel, D. (2013). Nutrients in the nation's waters: Too much of a good thing? Circular 1136. Reston, VA: U.S. Geological Survey. Retrieved from <http://pubs.usgs.gov/circ/circ1136/circ1136.html#FOREWORD>
- Mukundan, R., Pradhanang, S. M., Schneiderman, E. M., Pierson, D. C., Anandhi, A., Zion, M. S., ... Steenhuis, T. S. (2013). Suspended sediment source areas and future climate impact on soil erosion and sediment yield in a New York City water supply watershed. *Geomorphology*, 183(2013), 110-119. <http://dx.doi.org/10.1016/j.geomorph.2012.06.021>
- Nakicenovic, N., & Swart, R. (2000). Emissions scenarios: A special report of IPCC Working Group III. Geneva, Switzerland: Intergovernmental Panel on Climate Change.
- Nash, J. E., & Sutcliffe, J. V. (1970). River flow forecasting through conceptual models: Part I. A discussion of principles. *J. Hydrol.*, 10(3), 282-290. [http://dx.doi.org/10.1016/0022-1694\(70\)90255-6](http://dx.doi.org/10.1016/0022-1694(70)90255-6)
- Niraula, R., Kalin, L., Srivastava, P., & Anderson, C. J. (2013). Identifying critical source areas of nonpoint-source pollution with SWAT and GWLF. *Ecol. Model.*, 268, 123-133. <http://dx.doi.org/10.1016/j.ecolmodel.2013.08.007>

- Renkenberger, J. (2015). The impact of climate change on agricultural critical source areas (CSAs) and best management practices (BMPs) in eastern Maryland. MS thesis. College Park, MD: University of Maryland, Department of Civil and Environmental Engineering.
- Renkenberger, J., Montas, H., Leisnham, P., Chanse, V., Shirmohammadi, A., Sadeghi, A., ... Lansing, D. (2016). Comparison of SWAT predictions with stream biological integrity observations in an agricultural watershed. Presented at the ASABE 2016 Annual International Meeting. St. Joseph, MI: ASABE.
- Ritter, W. F., & Shirmohammadi, A. (2001). *Agricultural nonpoint-source pollution: Watershed management and hydrology*. Washington, DC: Lewis.
- Sexton, A. M., Sadeghi, A. M., Zhang, X., Srinivasan, R., & Shirmohammadi, A. (2010). Using NEXRAD and rain gauge precipitation data for hydrologic calibration of SWAT in a northeastern watershed. *Trans. ASABE*, 53(5), 1501-1510. <http://dx.doi.org/10.13031/2013.34900>
- Sexton, A. M., Shirmohammadi, A., Sadeghi, A. M., & Montas, H. J. (2011). A stochastic method to characterize model uncertainty for a nutrient TMDL. *Trans. ASABE*, 54(6), 2197-2207. <http://dx.doi.org/10.13031/2013.40659>
- Shang, X., Wang, X., Zhang, D., Chen, W., Chen, X., & Kong, H. (2012). An improved SWAT-based computational framework for identifying critical source areas for agricultural pollution at the lake basin scale. *Ecol. Model.*, 226, 1-10. <http://dx.doi.org/10.1016/j.ecolmodel.2011.11.030>
- Sohrabi, T. M., Shirmohammadi, A., Chu, T. W., Montas, H., & Nejadhashemi, A. P. (2003). Uncertainty analysis of hydrologic and water quality predictions for a small watershed using SWAT2000. *Environ. Forensics*, 4(4), 229-238. <http://dx.doi.org/10.1080/714044368>
- Teutschbein, C., & Seibert, J. (2012). Bias correction of regional climate model simulations for hydrological climate change impact studies: Review and evaluation of different methods. *J. Hydrol.*, 456-457, 12-29. <http://dx.doi.org/10.1016/j.jhydrol.2012.05.052>
- Van Liew, M. W., Feng, S., & Pathak, T. B. (2012). Climate change impacts on streamflow, water quality, and best management practices for the Shell and Logan Creek watersheds in Nebraska. *Intl. J. Agric. Biol. Eng.*, 5(1), 13-34.
- Wang, Y. (2015). A diagnostic decision support system for selecting best management practices in urban/suburban watersheds. PhD diss. College Park, MD: University of Maryland, Department of Civil and Environmental Engineering.
- Wang, Y., Montas, H. J., Brubaker, K. L., Leisnham, P. T., Shirmohammadi, A., Chanse, V., & Rockler, A. K. (2016). Impact of spatial discretization of hydrologic models on spatial distribution of nonpoint-source pollution hotspots. *J. Hydrol. Eng.*, 04016047. [http://dx.doi.org/10.1061/\(ASCE\)HE.1943-5584.0001455](http://dx.doi.org/10.1061/(ASCE)HE.1943-5584.0001455)
- White, M. J., Storm, D. E., Busteed, P. R., Stoodley, S. H., & Phillips, S. J. (2009). Evaluating nonpoint-source critical source area contributions at the watershed scale. *J. Environ. Qual.*, 38(4), 1654-1663. <http://dx.doi.org/10.2134/jeq2008.0375>
- White House. (2009). Executive Order 13508: Chesapeake Bay protection and restoration. Washington, DC: The White House. Retrieved from <https://www.whitehouse.gov/the-press-office/executive-order-chesapeake-bay-protection-and-restoration>
- Winchell, M. F., Folle, S., Meals, D., Moore, J., Srinivasan, R., & Howe, E. A. (2015). Using SWAT for sub-field identification of phosphorus critical source areas in a saturation excess runoff region. *Hydrol. Sci. J.*, 60(5), 844-862. <http://dx.doi.org/10.1080/02626667.2014.980262>
- Woznicki, S. A., & Nejadhashemi, A. P. (2012). Sensitivity analysis of best management practices under climate change scenarios. *JAWRA*, 48(1), 90-112. <http://dx.doi.org/10.1111/j.1752-1688.2011.00598.x>
- Woznicki, S. A., Nejadhashemi, A. P., & Smith, C. M. (2011). Assessing best management practice implementation strategies under climate change scenarios. *Trans. ASABE*, 54(1), 171-190. <http://dx.doi.org/10.13031/2013.36272>
- Yang, J., Reichert, P., Abbaspour, K. C., Xia, J., & Yang, H. (2008). Comparing uncertainty analysis techniques for a SWAT application to the Chaohe basin in China. *J. Hydrol.*, 358(1-2), 1-23. <http://dx.doi.org/10.1016/j.jhydrol.2008.05.012>